An Analytical Method To Predict Fatigue Life of Thermoplastics in Uniaxial Loading: Sensitivity to Wave Type, Frequency, and Stress Amplitude

Roel P. M. Janssen, Leon E. Govaert,* and Han E. H. Meijer

Materials Technology, Eindhoven University of Technology, P.O. Box 513, 5600 MB, Eindhoven, The Netherlands

Received June 8, 2007; Revised Manuscript Received January 22, 2008

ABSTRACT: A method is presented that allows fatigue life predictions on the basis of creep life data. The approach is based on the assumption that the time-dependent failure of polymers is determined by the intrinsic strain softening that is initiated when a critical threshold value of the plastic strain is surpassed. To facilitate fatigue predictions, an acceleration factor is defined that indicates how much faster plastic strain is accumulated by a cyclic signal compared to its static mean stress. Analytical solutions of the acceleration factor are presented for triangular and square waves, which predict that only the stress amplitude of the cyclic signal and the material's stress dependency affect fatigue life, whereas frequency plays no role. Verification using several glassy and semicrystalline polymers demonstrates that this method yields accurate quantitative lifetime predictions not only for polymers that exhibit ductile failure but also for those that display brittle fracture, provided that fracture is preceded by (localized) plastic flow.

I. Introduction

Constitutive equations have proven to be effective in describing large strain deformation of polymers.[1–5] Their significance was demonstrated by numerical studies that showed that polymer failure (e.g., via shear banding, necking, or crazing) is related to the polymer's intrinsic deformation behavior.[5–9] The true stress response (Figure 1a) is captured in constant strain rate tests in (uniaxial) compression, where localization phenomena are absent. The intrinsic deformation is initially (visco)elastic up to the yield point, followed by plastic deformation that shows strain softening and strain hardening. In tensile loading, intrinsic strain softening initiates strain localization, which rapidly develops until it is eventually stabilized by strain hardening.[7,8,10] From simulations it became evident that macroscopic ductile or brittle failure is controlled by the precise interplay between strain softening and strain hardening.[9,11]

In addition to predicting the response in short-term testing, the constitutive models were successfully employed to predict the polymer's lifetime under *constant stress*[12] and *cyclic stress.*[13] A justification is given in Figure 1b that shows the material's response for a constant true stress in compression, which illustrates that intrinsic deformation (strain softening followed by strain hardening) also plays a key role in the long-term failure of polymers.[12] After a load is applied in a constant-stress experiment, the polymer deforms at a constant strain rate until strain softening accelerates plastic deformation, upon which a plastic instability is formed that is stabilized by strain hardening with ongoing deformation. Since intrinsic strain softening plays a key role in the onset of polymer failure, Klompen et al.[14] incorporated an accurate description thereof in a pressure-modified Eyring equation. Since strain softening is independent of thermal history and temperature, it apparently always sets in at the same value of equivalent plastic strain: a critical plastic strain further referred to as ϵ_{cr}.

On the basis of these considerations, we hypothesize that the lifetime t_{fail} of a polymer under static or dynamic loading is only determined by a critical strain at which softening occurs, ϵ_{cr}, and the rate of accumulation of plastic strain $\dot{\epsilon}_{pl}(\sigma)$:

$$\epsilon_{cr} = \int_0^{t_{fail}} \dot{\epsilon}_{pl}(\sigma(t'))\, dt' \tag{1}$$

When an Eyring-type equation is used to describe plastic flow under static loading, the time-to-failure equals

$$t_{fail} = \frac{\epsilon_{cr}}{\dot{\epsilon}_{pl}(\sigma)} = \frac{\epsilon_{cr}}{\dot{\epsilon}_0 \sinh(\sigma/\sigma_0)} \approx \frac{2\epsilon_{cr}}{\dot{\epsilon}_0} \exp(-\sigma/\sigma_0) \tag{2}$$

Experimental observations by Crissmann and McKenna[15,16] confirm our hypothesis and relations comparable to eq 2 have been successfully applied to describe the time-dependent failure of different polymers subjected to dead weight loading.[17–22] Here it should be stressed that the physical interpretation of these models to describe failure is not always identical and we can distinguish (i) breakage of *primary* bonds and (ii) conformational changes/disruption of *secondary* (intermolecular) bonds. On the basis of these approaches, methods were proposed to allow fatigue life estimations based on (experimental) creep data by using a cumulative damage law.[18,23,24] Rather remarkable is that these methods predict a frequency-independent time-to-failure.

In this work we present an analytical method that is able to perform quantitative fatigue life predictions from a set of creep life data. This method predicts the initiation of crack growth, which is known to cover the majority (≥95%) of the total fatigue life.[25] It is in a manner similar to the cumulative damage law approaches mentioned.[18,23,24] However, our approach is based on the hypothesis that strain softening causes polymer failure and that it occurs when a critical value of plastic strain has developed (see Figure 1b). First, an analysis is presented that elaborates upon this hypothesis. It is based on the method developed to perform lifetime predictions under cyclic loading conditions and more specifically on how this method can be employed to grasp the influence of testing parameters like frequency, wave form, and stress amplitude. Subsequently, an attempt is made to characterize the relevant parameters for four different polymers. Equation 2 implies that stress-dependent creep (life) is governed by the same process as rate-dependent

* Corresponding author: Tel +31-402472838; Fax +31-402447355; e-mail l.e.govaert@tue.nl.

10.1021/ma071274a CCC: $40.75
Published on Web 03/12/2008

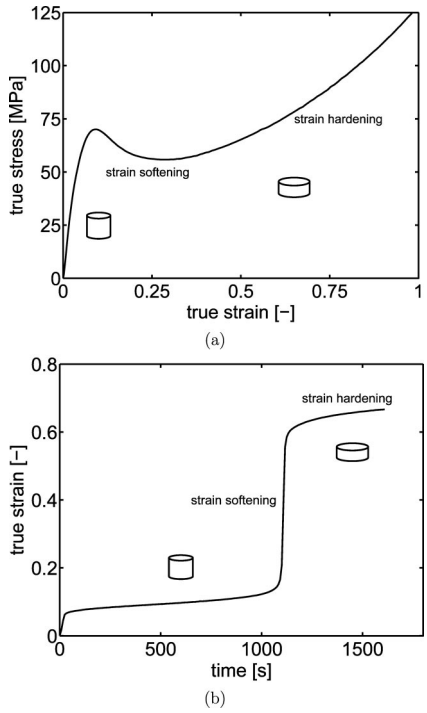

Figure 1. Intrinsic response of PC as obtained by compression testing at (a) *a constant true strain rate* and (b) *a constant true stress*. Reproduced with permission from ref 12. Copyright 2005 American Chemical Society.

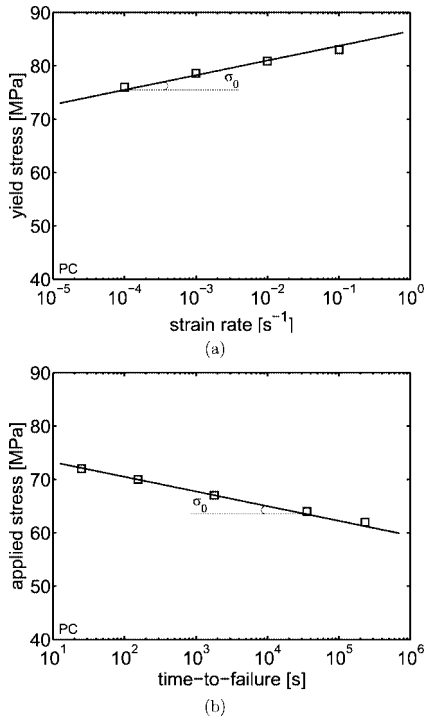

Figure 2. (a) Rate-dependent yield stress of PC in tension. (b) Stress-dependent time-to-failure of PC in tension. The slope of the solid line, though opposite in direction, is the same in both figures. Reproduced with permission from ref 12. Copyright 2005 American Chemical Society.

yielding. This is confirmed for polycarbonate (PC) by experimental results of Klompen et al.[12] (see Figure 2) and by findings of Bauwens-Crowet et al.[22] The model developed is verified in fatigue experiments on all four polymers used, which encompass two glassy polymers that fail either ductile or brittle, and two semicrystalline polymers that display ductile failure.

II. Experimental Section

A. Materials. The materials used are polycarbonate (PC) (Lexan 161R, GE Plastics), poly(methyl methacrylate) (PMMA) (Plexiglas V826, Röhm GmbH), high-density polyethylene (HDPE) (Stamylan HD9089, DSM), and an isotactic polypropylene (iPP) (Stamylan P13e10, DSM). Granules of these materials were injection-molded into tensile bars: PC, PMMA, and iPP were 3.2 mm thick and satisfied the ASTM-D638 norm, while the geometry of the 4 mm thick HDPE bars was according to ISO-527. To mitigate stress accelerated physical aging during testing,[14] the PC samples were annealed for 72 h at 120 °C.

B. Mechanical Testing. All mechanical tests were performed on a servo-hydraulic MTS Testing System 810 in a temperature chamber at 20 °C. Prior to testing, the samples were allowed to acclimatize for at least 15 min. Tensile tests were performed at constant linear strain rates in a range from 10^{-4} to 10^{-2} s^{-1}. Creep and fatigue tests were conducted under load control. Per series of tests, typically the stress amplitude of the signal was kept constant, whereas the mean stress was varied. Various stress signals were applied: square-, triangular-, and sinusoidal-shaped signals and arbitrary signals consisting of combinations of these wave forms. The frequencies applied fell within the range of 1−10 Hz. At least two experiments were performed per test condition.

III. An Analysis to the Time-Dependent Fatigue Failure

Outside the laboratory environment, complex geometries, nonisothermal conditions, and possibly physical aging or secondary crystallization complicate predictions on deformation and failure of polymers. Therefore, models that describe the rate of accumulation of plastic strain necessarily must be more complex than the one used in eq 2. An onset for such a formulation was already successfully derived in models that describe the plastic flow of polymers[12–14] and reads

$$\dot{\epsilon}_{pl} = \underbrace{\dot{\gamma}_0^*(T)\cdot\sinh\left(\frac{\bar{\tau}}{\tau_0}\right)}_{\text{(I)}}\cdot\underbrace{\exp\left(\frac{-\mu p}{\tau_0}\right)}_{\text{(II)}}\cdot\underbrace{\exp\left(-S(t,T,\bar{\tau})\right)}_{\text{(III)}} \tag{3}$$

where

$$\dot{\gamma}_0^* = \dot{\gamma}_0\exp\left(\frac{-\Delta U}{RT}\right)\ \text{and}\ \ \tau_0 = \frac{kT}{V^*} \tag{4}$$

The temperature and stress dependence is captured in part I, where $\bar{\tau}$ is the equivalent stress, $\dot{\gamma}_0$ a constant, ΔU the activation energy, V^* the activation volume, R the universal gas constant, k Boltzmann's constant, and T the absolute temperature. Part II covers the effect of the loading geometry, with μ the pressure dependency and p the hydrostatic pressure. The effect of physical aging is dealt with in part III, where the state parameter S describes the softening behavior that depends on the thermo-mechanical history and aging, also during the experiment.[14]

The analysis presented here is restricted to uniaxial tensile loading under isothermal conditions, without the presence of physical aging during loading, which reduces eq 3 to

$$\dot{\epsilon}_{\text{pl}} \approx \frac{\dot{\epsilon}_0}{2}\exp\left(\frac{\sigma(t)}{\sigma_0}\right) \tag{5}$$

with $\dot{\epsilon}_0$ a rate constant, $\sigma(t)$ the stress signal applied, and σ_0 a characteristic stress. Note that

$$\dot{\epsilon}_0 = \frac{\dot{\gamma}_0^*(T)\exp(S_a)}{\sqrt{3}}\ \ \text{and}\ \ \sigma_0 = \frac{3\tau_0}{\sqrt{3}+\mu} \tag{6}$$

The analysis starts from the hypothesis that strain softening initiates fatigue failure and occurs at the moment that a critical value of plastic strain, ϵ_{cr}, has accumulated. As a consequence,

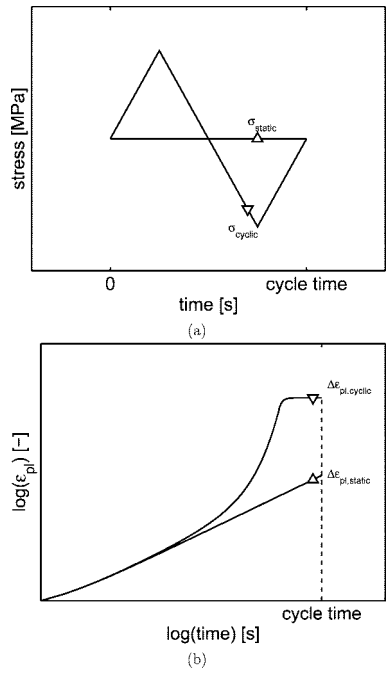

Figure 3. (a) One cycle of a triangular-shaped stress signal σ_{cyclic} and its mean stress σ_{static}. (b) Development of plastic strain during one cycle of the signals in Figure 3a calculated using eq 5.

the rate at which plastic strain accumulates, $\dot{\epsilon}_{pl}$, is the decisive factor in determining the time-to-failure, t_{fail}, of polymers:

$$\epsilon_{cr} = \int_0^{t_{fail}} \dot{\epsilon}_{pl}(\sigma(t'))\, dt' = \int_0^{t_{fail}} \dot{\epsilon}_0 \sinh\left(\frac{\sigma(t')}{\sigma_0}\right) dt' \tag{7}$$

In the case of constant stress loading, eq 7reduces to an expression for the time-to-failure given by

$$t_{fail} = \frac{\epsilon_{cr}}{\dot{\epsilon}_{pl}(\sigma_{static})} = \frac{\epsilon_{cr}}{\dot{\epsilon}_0 \sinh\left(\frac{\sigma_{static}}{\sigma_0}\right)} \tag{8}$$

This equation shows that, besides the stress applied, only three *material* parameters affect the lifetime under a static stress: a rate constant $\dot{\epsilon}_0$, a characteristic stress σ_0, and the critical value of plastic strain at which softening of the material starts ϵ_{cr}. The first two parameters are obtained from the strain rate dependence of the yield stress using eq 5, as shown for PC in Figure 2a, where the slope of the curve is equal to ln(10) σ_0. The latter parameter is obtained from creep life data, as shown for PC in Figure 2b, using eq 8. In arbitrary 3D loading situations, a similar result can be obtained by defining a critical equivalent plastic strain $\bar{\gamma}_{cr}$ and describing the plastic flow in equivalent terms (see eq 3).

For materials that fail brittle, usually fracture occurs prior to reaching the macroscopic yield stress in tensile tests[31] and, as a result, the parameters $\dot{\epsilon}_0$ and σ_0 cannot be derived from yield stress data. Rewriting eq 8

$$t_{fail} = \frac{t_0}{\sinh\left(\frac{\sigma_{static}}{\sigma_0}\right)} \tag{9}$$

where

$$t_0 = \frac{\epsilon_{cr}}{\dot{\epsilon}_0} \tag{10}$$

solves the problem, since the parameter σ_0 (also) represents the stress dependence of the time-to-failure under static loading,[12,22] as shown in Figure 2b. Both unknowns, t_0 and σ_0, can be derived from creep life data only. It is underlined though that when possible it is preferred to determine the parameters $\dot{\epsilon}_0$ and ϵ_{cr} rather than t_0, since they can be translated to perform lifetime predictions in arbitrary 3D loading geometries.

The effect of the type of cyclic stress signal used on time-to-failure is analyzed by comparing its influence on the rate of accumulation of plastic strain to that of its (static) mean stress, applying eq 5 using first a triangular wave form as an example (see Figure 3a). Figure 3b shows that more plastic strain is accumulated in cyclic loading; thus, a cyclic stress accelerates the accumulation of plastic strain in comparison to its static mean stress by an *acceleration factor* a_{cyclic}:

$$a_{cyclic} = \frac{\int_0^{t_{cycle}} \dot{\epsilon}_{pl}(\sigma_{cyclic}(t'))\, dt'}{\int_0^{t_{cycle}} \dot{\epsilon}_{pl}(\sigma_{static})\, dt'} \tag{11}$$

Provided that the critical plastic strain at which failure occurs, ϵ_{cr}, is identical under static and cyclic loading, we can write, using eq 8:

$$t_{fail,cyclic} = \frac{t_{fail,static}(\sigma_{static})}{a_{cyclic}} = \frac{\epsilon_{cr}}{\dot{\epsilon}_0 \sinh\left(\frac{\sigma_{static}}{\sigma_0}\right) a_{cyclic}} \tag{12}$$

or with only creep data available, using eq 9:

$$t_{fail,cyclic} = \frac{t_{fail,static}(\sigma_{static})}{a_{cyclic}} = \frac{t_0}{\sinh\left(\frac{\sigma_{static}}{\sigma_0}\right) a_{cyclic}} \tag{13}$$

The acceleration factor can be obtained for any dynamic signal by solving the integrals in eq 11. Analytical solutions are presented for a triangular wave (see Figure 4a and the Appendix):

$$a_{tria}(\sigma_{ampl}) = \frac{\sinh\left(\frac{\sigma_{ampl}}{\sigma_0}\right)}{\frac{\sigma_{ampl}}{\sigma_0}} \tag{14}$$

and a square wave (see Figure 4b and the Appendix):

$$a_{sq}(\sigma_{ampl}) = \cosh\left(\frac{\sigma_{ampl}}{\sigma_0}\right) \tag{15}$$

Strikingly, for a given wave form only one parameter accelerates the rate of accumulation of plastic strain with respect to the mean stress of the signal: the ratio of the testing parameter σ_{ampl} and the material parameter σ_0. In addition, frequency has no effect on the fatigue lifetime, which is in agreement with other fatigue analyses.[18,23,24]

Figure 5a elucidates the method to perform cyclic fatigue life predictions by shifting a set of creep life data along the time axis. The magnitude of the horizontal shift a_{cyclic} depends on the ratio of the stress amplitude σ_{ampl} applied, the material's stress dependence σ_0, and the wave form applied only.

Using the value of σ_0 from ref 14, the acceleration factors of a square, triangular, and sine wave (the last one obtained via numerical integration) are calculated for PC and plotted as a function of amplitude in Figure 5b. A square wave has the largest acceleration factor, developing more plastic strain during a cycle than a sine wave and a triangular wave with the same stress amplitude. This is in line with eq 5 which indicates an exponential increase of plastic flow rate with increasing stress as well as with experimental findings.[26–28] To illustrate the

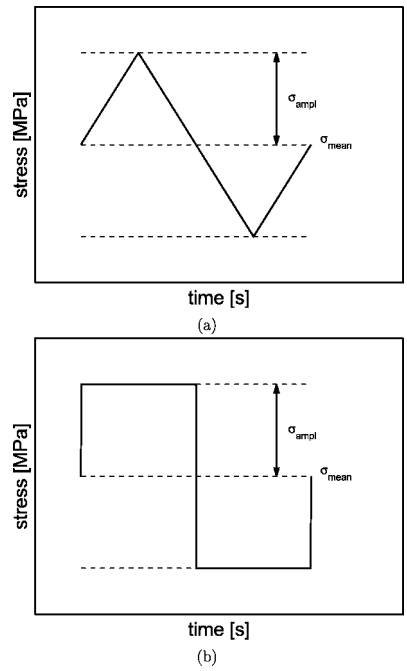

Figure 4. (a) A triangular stress signal and (b) a square stress signal, both defined by a mean stress σ_{mean} and a stress amplitude σ_{ampl}.

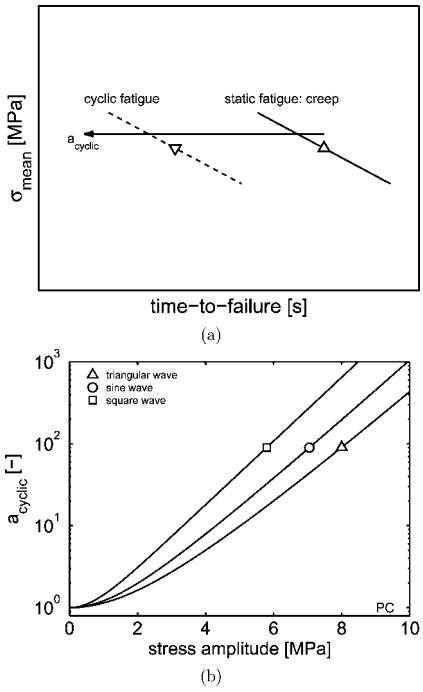

Figure 5. (a) Schematic representation of the applicability of the acceleration factor σ_{cyclic} to perform lifetime predictions of cyclic fatigue from time-to-failure data under static fatigue. (b) Influence of stress amplitude on the acceleration factor of PC for three wave forms.

influence of the stress amplitude and the wave form on time-dependent failure, cyclic fatigue life predictions are performed on the basis of lifetime data of annealed PC samples under static loading from ref 12, using a_{cyclic} from Figure 5b and eq 13. Figure 6a shows the decrease in fatigue life with increasing amplitude, and Figure 6b shows the influence of the wave forms.

IV. Fatigue Failure: Materials Characterization

The analytical considerations presented in the previous section revealed that only three *material* parameters are required to

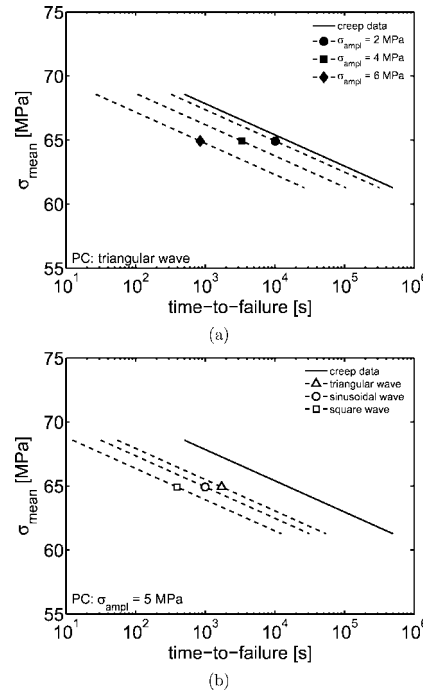

Figure 6. Illustration of the influence of (a) stress amplitude and (b) wave form (square, sinusoidal, and triangular) on the fatigue life using eq 13. The parameters set used is that of PC taken from ref 14.

describe the creep life of polymers: a rate constant $\dot{\epsilon}_0$, a characteristic stress σ_0, and the critical value of plastic strain at which softening of the material is initiated ϵ_{cr}. In this section, an attempt is made to obtain these parameters for four polymers differing in macroscopic ductility and crystallinity: PC, HDPE, iPP, and PMMA.

Figure 7a shows the yield stress vs the strain rate of PC obtained by tensile testing (symbols). The solid line is the Eyring flow equation fit, eq 5, yielding values of $\dot{\epsilon}_0 = 1.2 \times 10^{-29}$ s^{-1} and $\sigma_0 = 1.19$ MPa.

Figure 7b shows the lifetime of PC when subjected to a constant (tensile) stress, defining time-to-failure as the moment of neck formation. The value $\epsilon_{cr} = 0.007$ is found by fitting eq 8 to these data using $\dot{\epsilon}_0$ and σ_0 just obtained.

Figure 8a displays the creep life data of PMMA, which is, in contrast to PC, a polymer glass that fractures at failure. In this specific case the samples only displayed a yield stress at strain rates below 10^{-4} s^{-1}. In all creep tests the PMMA samples remain optically flawless (no visible crazing) until they fracture, and only a single fatal crack is found with no significant plastic strain localization visual around the point of failure. To demonstrate that, despite the brittle fracture observed in PMMA, failure is also in this case preceded by bulk plastic deformation, we use the creep data to construct constructed a so-called Sherby−Dorn plot[57] (see Figure 8b), in which the logarithm of the creep rate is plotted as a function of creep strain. For all stress levels an initial decrease of the creep rate with deformation is found; this is the so-called primary creep stage. Subsequently, the creep rate reaches a minimum, commonly referred to as the plateau creep rate representing the secondary creep stage of plastic flow. Similar to the completely ductile materials, the resulting flow rate strongly depends on applied stress. Finally, as a result of intrinsic and geometric softening, the strain rate increases again (tertiary creep) until failure occurs. For all loads studied, the PMMA samples reached the plastic flow stage before fracture occurs. To characterize the stress dependence of plastic flow, the plateau creep rate (minimum rate in static loading) is plotted versus the applied stress in Figure 9. This

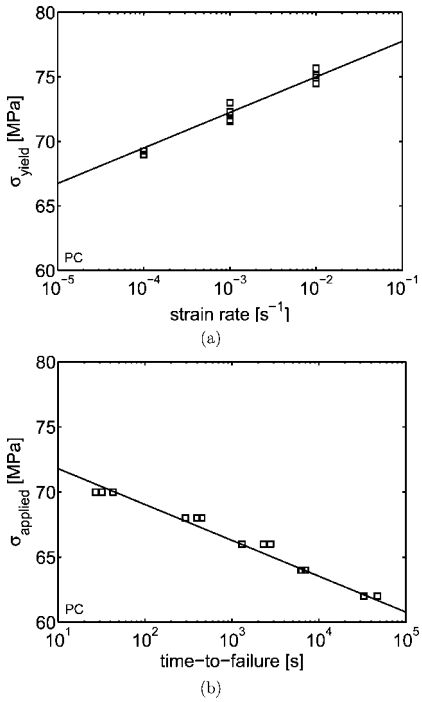

Figure 7. (a) Yield stress vs strain rate in tension and (b) applied stress vs time-to-failure in tensile creep for PC (Lexan 161R). The number of decades on the abscissa and scale on the ordinate are equal in both figures. Solid lines are fits using eqs 5 and 8 with the parameter values of Table 1.

Table 1. Material Parameters Obtained from Tensile Testing (σ_0 and $\dot{\epsilon}_0$) or Creep Testing (σ_0 and ϵ_{cr}) for All Polymers Used in This Study

	PC	HDPE	iPP	PMMA
σ_0 [MPa]	1.19	1.96	1.70	3.65
$\dot{\epsilon}_0$ [s^{-1}]	1.20×10^{-29}	1.12×10^{-8}	1.95×10^{-12}	4×10^{-12}
ϵ_{cr}	0.007	0.139	0.0873	0.065

plot, which is equivalent to a plot of yield stress versus strain rate,[58] shows a change in slope within the range of loads applied, revealing the thermorheologically complex behavior of PMMA, which is notably reflected in a change in the slope of the strain rate dependence of the yield stress.[29] This complex behavior can be accurately described using the Ree−Eyring approximation,[30] where it is assumed that two stress-activated processes act in parallel. At low rates we only find main-chain segmental motion, the α-process, and at high rates, the secondary glass transition originating from either a side-group motion or partial mobility of the main chain, the β-process. At low strain rates (relevant for this study) the β-process does not contribute, and we therefore only derived the Eyring flow parameters of the primary α-process, represented by the solid lines in both Figures 8a and Figure 9. Both are described well by the values of $\sigma_0 = 3.65$ MPa, $\dot{\epsilon}_0 = 4 \times 10^{-12}$ s^{-1}, and $\epsilon_{cr} = 0.065$.

Now we turn to semicrystalline polymers. Given the same slopes, be it with opposite sign in Figures 7a,b and 8a,b, experimental proof exists that σ_0 determines the rate dependence of the yield stress as well as the stress dependence of the creep life, in accordance with eq 8. This result is now verified for semicrystalline polymers that also fail ductile by neck formation: HDPE and iPP. Figure 10a shows the yield stress in tension vs the strain rate for HDPE and iPP, while in Figure 10b the time-to-failure as a function of the applied tensile stress is plotted. The range of the scales on the axes is identical in both graphs and a line is fitted through the experimental data using eqs 5 and 8. In correspondence with the results obtained for PC, the slope of the solid lines is the same in both plots for both HPDE and iPP. The values derived for $\dot{\epsilon}_0$, σ_0, and ϵ_{cr} are tabulated in Table 1.

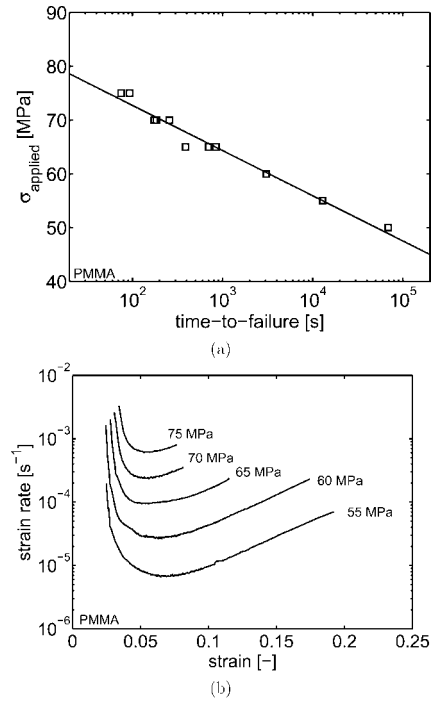

Figure 8. (a) Applied stress vs time-to-failure for PMMA in tensile creep. The solid line is a fit using eq 8 with the parameter values of Table 1. (b) Applied stress versus creep rate for PMMA in uniaxial creep loading at various stress levels (so-called Sherby−Dorn plots).

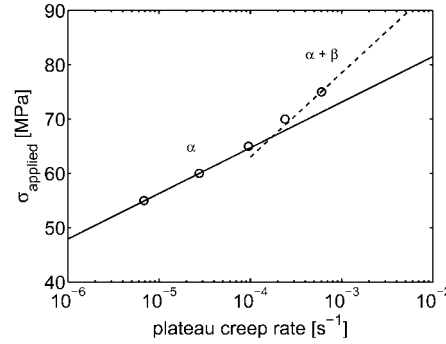

Figure 9. Applied stress in creep testing vs the plateau creep rate for PMMA. The solid line is a fit using eq 5 with the parameter values of Table 1.

V. Fatigue Failure: Validation

A. Effect of Stress Amplitude. To validate the applicability of the acceleration factor as a method to predict the fatigue life, experiments were carried out with various stress amplitudes, wave forms, and frequencies. First, the effect of amplitude is investigated by subjecting the polymers to a triangular wave with an amplitude of 5 or 10 MPa at a frequency of 1 Hz, selected to minimize the effect of dissipative heating.

The symbols in Figure 11a denote the lifetime of PC subjected to static (creep) and cyclic stress. Clearly, the lifetime decreases significantly with increasing stress amplitude. Lifetime predictions are performed with eq 12, using the acceleration factor of a triangular wave (eq 14) and the parameter values for PC given in Table 1. The predictions (dashed lines) show a clear overlap with experiments in the high stress range, demonstrating that the approach employed is effective. The mismatch at lower stresses is most likely related to physical aging that is known

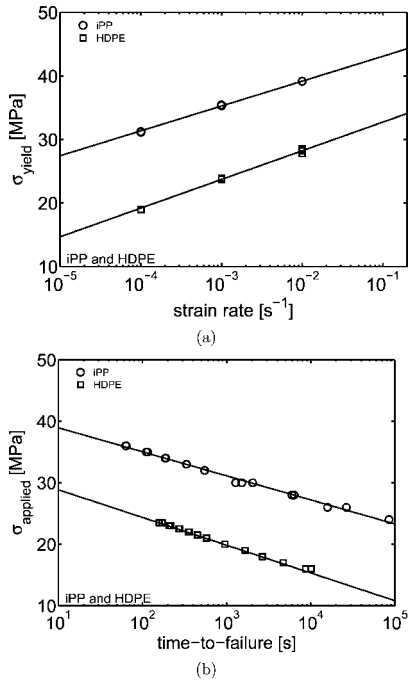

Figure 10. As Figure 7, now for HDPE (Stamylan HD9089, squares) and iPP (Stamylan P13e10, circles).

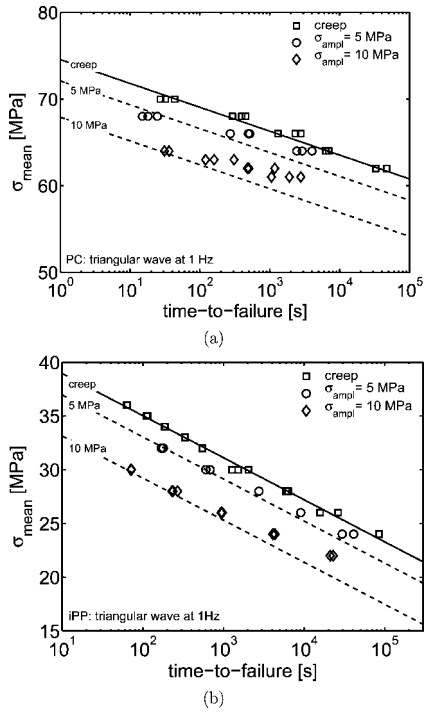

Figure 11. Applied stress vs time-to-failure for (a) PC (Lexan 161R) and (b) iPP (Stamylan P13e10). Symbols represent experiments (creep: squares; triangular wave 5 MPa: circles; 10 MPa: diamonds), whereas the dotted lines are fatigue predictions according to eq 12.

to have a prolonging effect on the lifetime of PC[12,13] accompanied by an increase in yield stress.[13,14] This is completely in line with studies that reported effects of physical aging during fatigue loading of glassy polymers.[32–37] Apparently, the annealing procedure to mitigate physical aging was insufficient within the time range studied.

HDPE and iPP samples are tested to validate the applicability of the acceleration factor to semicrystalline polymers. Again, eq 12 is used to predict the time-to-failure, since both materials

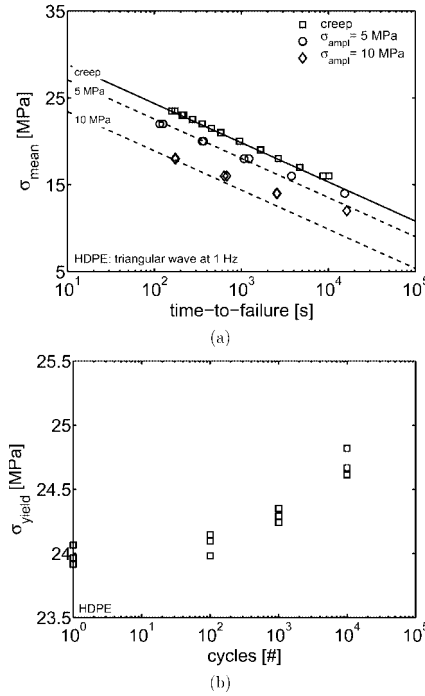

Figure 12. (a) As Figure 11, now for HDPE (Stamylan HD9089). (b) Evolution of the yield stress of HDPE during cyclic fatigue. A triangular wave of 1 Hz was applied with a mean stress of 12 MPa and an amplitude of 10 MPa.

fail by neck formation. The results in Figures 11b and 12a show that accurate predictions are acquired over a wide range of (mean) stresses for the signal with an amplitude of 5 MPa, whereas for 10 MPa, adequate predictions are obtained only in the high mean stress range. With decreasing stress, a similar divergence between prediction and experiment is observed as for PC, possibly related to time-dependent microstructural changes due to physical aging.[38–40] Since for PC this deviation was accompanied by an increase in yield stress,[13] an examination is performed on the evolution of the yield stress of HDPE during fatigue loading by loading.

Samples are loaded at a mean stress of 12 MPa and an amplitude of 10 MPa for 10^2, 10^3, and 10^4 s, which is below the time-to-failure observed ($\sim 2 \times 10^4$ s). Subsequently, a tensile test is performed on the samples at a strain rate of 10^{-3} s^{-1}. The results in Figure 12b show a significant increase in yield stress with prolonged fatigue loading. Though an investigation to the precise underlying (microstructural) mechanisms lies beyond the scope of this work, the results are in full agreement with observations that suggest fatigue induced (microstructural) changes in heterogeneous polymer systems.[41–46]

B. Effect of Wave Form. PMMA samples are subjected to a triangular wave and a square wave with an amplitude of 10 MPa at a frequency of 1 Hz to investigate whether the acceleration factor covers the effect of wave form. Fatigue life predictions are performed according to eq 12, using eqs 14 and 15 to determine the value of both acceleration factors together with the values of σ_0, $\dot{\epsilon}_0$, and ϵ_{cr} for PMMA as provided in Table 1.

Figure 13 shows that the method provides quantitative and accurate time-to-failure predictions for both wave forms. It can also be seen that the lifetime is lower under a square wave than under a triangular wave, which is in line with the analysis. Moreover, the observed failure is brittle fracture, and therefore the results support the hypothesis that the lifetime of materials that fail brittle as well as of those that fail ductile (PC, HDPE,

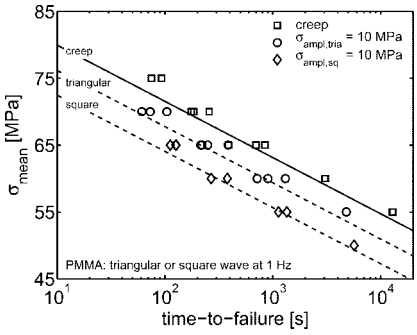

Figure 13. Applied stress vs time-to-failure for PMMA (Plexiglas V826). Symbols represent experiments (creep: squares; triangular wave 10 MPa: circles; square wave 10 MPa: diamonds). The dotted lines are fatigue predictions according to eq 13.

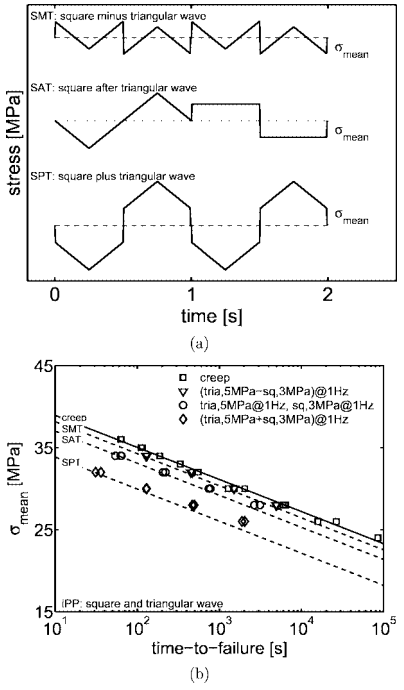

Figure 14. (a) Stress signals applied to iPP (Stamylan P13e10). (b) Applied stress vs time-to-failure of iPP subjected to the signals (a). Symbols represent experiments, whereas the dotted lines are the fatigue predictions according to eq 12.

iPP) is governed by intrinsic strain softening, as long as failure is dominated by localized plastic flow.

More complex wave forms are applied to iPP and are composed of a 1 Hz square wave with an amplitude of 3 MPa and a 1 Hz triangular wave with an amplitude of 5 MPa (see Figure 14a). Also for these complex wave forms the lifetime predictions as obtained by eq 12 agree precisely with experiments (see Figure 14b). The acceleration factor of signals composed of different subsequent contributions, like the SAT signal (square after triangular wave) in Figure 14a, are given by

$$a_{\text{cyclic}} = \sum_{i=1}^{n} \frac{t_i}{t_{\text{cycle}}} a_i \tag{16}$$

with n the number of signals, t_i the cycle time of the ith signal, t_{cycle} the cycle time of the total signal, and a_i the acceleration factor of each signal. In this case, the acceleration factor of the individual signals can be obtained analytically. Also the SMT and SPT signals (square minus triangular and square plus triangular, respectively; see Figure 14a) yield analytical solutions for the acceleration factor:

$$a_{\text{SMT}} = \frac{\sinh\left(\dfrac{\sigma_{\text{ampl,sq}}}{\sigma_0}\right) + \cosh\left(\dfrac{\sigma_{\text{ampl,sq}} - \sigma_{\text{ampl,tria}}}{\sigma_0}\right)}{\dfrac{\sigma_{\text{ampl,tria}}}{\sigma_0}} \tag{17}$$

$$a_{\text{SPT}} = \frac{\cosh\left(\dfrac{\sigma_{\text{ampl,sq}}}{\sigma_0}\right) + \sinh\left(\dfrac{\sigma_{\text{ampl,sq}} + \sigma_{\text{ampl,tria}}}{\sigma_0}\right)}{\dfrac{\sigma_{\text{ampl,tria}}}{\sigma_0}} \tag{18}$$

To challenge the performance of our method even further, the complexity of the wave form applied is increased by combining a 4 Hz sinusoidal shaped wave with an amplitude of 3 MPa, a 1 Hz square wave with an amplitude of 2 MPa, and a 3 Hz triangular wave with an amplitude of 5 MPa either positioned consecutively, referred to as the SST signal (sinusoidal, square, triangular), or merged into one signal, referred to as the random signal (see Figure 15a). The sinusoidal-shaped wave in these signals requires numerical integration of eq 11 to obtain the correct acceleration factor. Figure 15b indicates that all predictions accurately cover the experiments, and it is evident that the concept of an acceleration factor could be effective for *any* repeating dynamic signal.

C. Effect of Frequency. A remarkable outcome of the analysis is that the frequency applied does not affect the fatigue life under isothermal conditions. This is experimentally checked on iPP using a triangular-shaped stress signal with an amplitude of 5 or 10 MPa. In Figure 11b it was shown that the fatigue life predictions for iPP were accurate, and these experimental results at 1 Hz are combined with data obtained at frequencies of 2, 5, and 10 Hz in Figure 16a. Regarding the samples fatigued at an amplitude of 5 MPa, the applied frequency indeed has no influence on the fatigue life, despite an order of magnitude difference in frequency, which is in full accordance with data from literature in this frequency range.[27,47] However, fatigue life data obtained at frequencies below this range indicate an effect of frequency.[24,27] The frequency applied also appears to

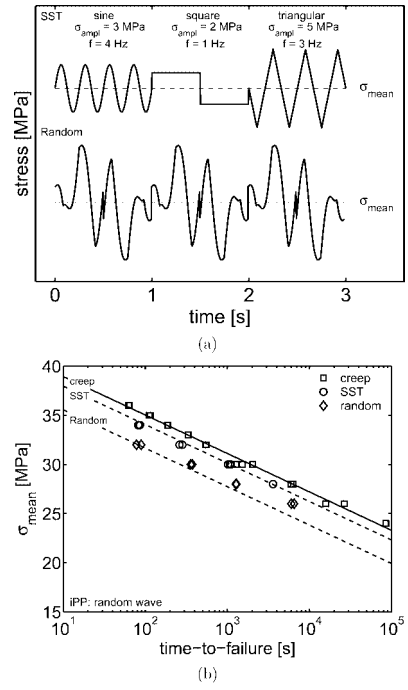

Figure 15. (a) Stress signals applied to iPP (Stamylan P13e10). (b) Applied stress vs time-to-failure of iPP subjected to the "complex" signals (a). Symbols represent experiments, whereas the dotted lines are the fatigue predictions according to eq 12.

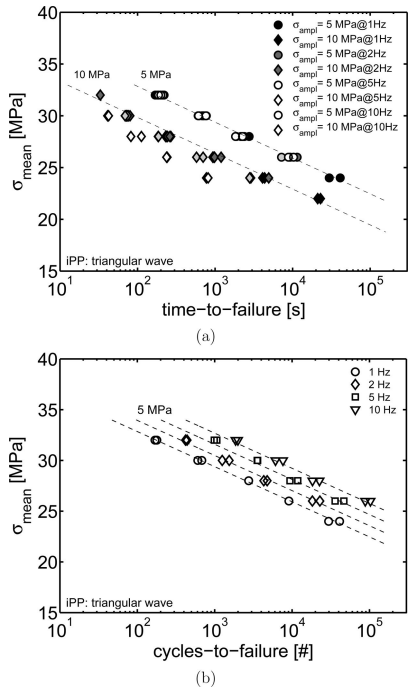

Figure 16. (a) Applied stress vs time-to-failure for iPP (Stamylan P13e10) subjected to a triangular wave with an amplitude of 5 or 10 MPa and a frequency of 1, 2, 5, or 10 Hz. (b) Data of 5 MPa plotted now vs cycles-to-failure. The lines are a guide to the eye.

have an effect on the time-to-failure of the signal with a stress amplitude of 10 MPa, in particular at higher frequencies (see Figure 16a). It is well-established that polymers dissipate a substantial amount of energy at high stress[48–53] and high frequency,[53–56] which causes substantial heating of the sample as also demonstrated in ref 13. For that reason, a frequency dependence may be anticipated at higher amplitudes, where hysteretic heating is more likely to occur. Nonetheless, the experimental results endorse that failure of polymers is independent of frequency, provided that isothermal conditions prevail. Figure 16b plots the fatigue life of the samples subjected to an amplitude of 5 MPa in cycles-to-failure instead of time-to-failure. Also, this plot indicates a direct relation between the number of cycles-to-failure and frequency, but since it is proven that polymer fatigue failure is independent of frequency, it is demonstrated that the *time-to-failure* rather than *cycles-to-failure* must be used to analyze fatigue life data in the most simple and effective way.

VI. Conclusions

A method is proposed to predict the time-dependent failure of polymers. It assumes that polymer failure is governed by the onset of intrinsic strain softening, which is triggered when a critical value of the plastic strain ϵ_{cr} is reached. This indicates that polymer lifetime depends mainly on the rate by which plastic strain is accumulated, which can be expressed by an Eyring flow equation that requires two parameters, besides the applied stress σ: a rate constant $\dot{\epsilon}_0$ and the stress dependency σ_0. Tensile and creep experiments were performed on four different polymers (PC, PMMA, HDPE, and iPP) to obtain the relevant parameters, and it is proven that they accurately describe the lifetime of these polymers under static (creep) loading.

An acceleration factor that relates the plastic strain developed during a cycle of a repeating dynamic signal to that of its (static) mean stress has been defined to capture the effect of cyclic fatigue on the time-dependent failure of polymers. This acceleration factor is a measure of how much faster plastic strain is accumulated compared to its static mean stress, and it can thus be employed to perform fatigue life predictions (see eqs 12 and 13). Analytical solutions are presented for a square and triangular wave, which suggest that under isothermal conditions only the ratio of two parameters influences the fatigue life of polymers: the stress amplitude σ_{ampl} and the material's stress dependence σ_0. Strikingly, frequency plays no role. An analysis of the influence of independent fatigue testing parameters, such as stress amplitude, wave form, and frequency, indicated that a square wave has a higher acceleration of plastic flow (in comparison to the mean stress) than a sinusoidal or triangular wave. It is proven that the method proposed yields accurate quantitative lifetime predictions. This has been validated on all polymers used in this study. Moreover, fatigue testing on iPP indeed indicates that the frequency applied has no effect on the time-to-failure, provided that isothermal conditions prevail.

Besides the hysteretic heating effects observed for iPP at high amplitudes and frequencies, the analysis does not account yet for physical aging during the experiment, which causes a divergence between the predicted and experimentally obtained lifetime of PC at lower stresses (longer times). Remarkably, similar effects are perceived for the semicrystalline polymers HDPE and iPP, and moreover, it was proven that the yield stress of HDPE increases during fatigue loading, analogous to physical aging of PC. However, an explanation for these observations is beyond the scope of this work.

We believe that we have proven that the lifetime of polymers under static or dynamic loading is determined by the time-dependent accumulation of plastic strain and that failure takes place at the moment a critical value of plastic strain is surpassed that initiates strain softening. Accurate lifetime estimations were obtained by an analysis based on these assumptions.

Acknowledgment. The authors acknowledge the financial support provided by the Dutch Polymer Institute (DPI Project 445).

Appendix

Acceleration Factor of a Triangular Wave. The acceleration factor of a cyclic signal is defined as

$$a_{cyclic} = \frac{\int_0^{t_{cycle}} \dot{\epsilon}_{pl,cyclic}\, dt}{\int_0^{t_{cycle}} \dot{\epsilon}_{pl,static}\, dt} = \frac{\Delta\epsilon_{pl,cyclic}}{\Delta\epsilon_{pl,static}} \tag{19}$$

The plastic strain accumulated during a cycle can be determined by integration of the Eyring flow equation, which relates the stress σ to the plastic strain rate $\dot{\epsilon}_{pl}$. Under uniaxial, isothermal conditions and at large stresses, this equation is given by

$$\dot{\epsilon}_{pl}(\sigma) = \dot{\epsilon}_0 \exp\left(\frac{\sigma}{\sigma_0}\right) \tag{20}$$

where σ is the uniaxial stress, σ_0 is a characteristic stress, and $\dot{\epsilon}_0$ equals

$$\dot{\epsilon}_0 = \dot{\epsilon}_0^* \exp\left(\frac{-\Delta U}{RT}\right) \tag{21}$$

with $\dot{\epsilon}_0^*$ a constant, ΔU the activation energy, R the gas constant, and T the absolute temperature.

To calculate the total accumulated plastic strain per cycle of a triangular wave $\Delta\epsilon_{pl,cyclic}$, the stress signal is divided into three parts:

$$0 \le t < \frac{1}{4f}: \qquad \sigma = \sigma_{mean} + 4f\sigma_{ampl}t$$

$$\frac{1}{4f} \le t < \frac{3}{4f}: \qquad \sigma = \sigma_{mean} + 2\sigma_{ampl} - 4f\sigma_{ampl}t$$

$$t\frac{3}{4f} \le t < \frac{1}{f}: \qquad \sigma = \sigma_{mean} - 4\sigma_{ampl} + 4f\sigma_{ampl}t \quad (22)$$

where f is the frequency, σ_{mean} is the mean stress, σ_{ampl} is the stress amplitude, and t is the elapsed time.

For each part, the accumulated plastic strain can be determined by integration of eq 20:

$$\begin{aligned}\Delta\epsilon_{pl,1} &= \int_0^{1/4f} \frac{1}{2A_{rej}} \exp\left[\frac{\sigma_{mean} + 4f\sigma_{ampl}t}{\sigma_0}\right] dt \\ &= \frac{1}{2A_{rej}} \exp\left[\frac{\sigma_{mean}}{\sigma_0}\right] \int_0^{1/4f} \exp\left[\frac{4f\sigma_{ampl}t}{\sigma_0}\right] dt \\ &= \dot{\epsilon}_{pl}(\sigma_{mean}) \int_0^{1/4f} \exp\left[\frac{4f\sigma_{ampl}t}{\sigma_0}\right] dt \\ &= \dot{\epsilon}_{pl}(\sigma_{mean}) \left[\frac{\sigma_0}{4f\sigma_{ampl}} \exp\left[\frac{4f\sigma_{ampl}t}{\sigma_0}\right]\right]_0^{1/4f} \\ &= \dot{\epsilon}_{pl}(\sigma_{mean}) \frac{\sigma_0}{4f\sigma_{ampl}} \left(\exp\left[\frac{\sigma_{ampl}}{\sigma_0}\right] - 1\right) \end{aligned} \quad (23)$$

$$\begin{aligned}\Delta\epsilon_{pl,2} &= \int_{1/4f}^{3/4f} \frac{1}{2A_{rej}} \exp\left[\frac{\sigma_{mean} + 2\sigma_{ampl} - 4f\sigma_{ampl}t}{\sigma_0}\right] dt \\ &= \dot{\epsilon}_{pl}(\sigma_{mean}) \frac{\sigma_0}{4f\sigma_{ampl}} \exp\left[\frac{2\sigma_{ampl}}{\sigma_0}\right] \left(\exp\left[\frac{-\sigma_{ampl}}{\sigma_0}\right] - \exp\left[\frac{-3\sigma_{ampl}}{\sigma_0}\right]\right) \end{aligned} \quad (24)$$

$$\begin{aligned}\Delta\epsilon_{pl,3} &= \int_{3/4f}^{1/f} \frac{1}{2A_{rej}} \exp\left[\frac{\sigma_{mean} - 4\sigma_{ampl} + 4f\sigma_{ampl}t}{\sigma_0}\right] dt \\ &= \dot{\epsilon}_{pl}(\sigma_{mean}) \frac{\sigma_0}{4f\sigma_{ampl}} \exp\left[\frac{-4\sigma_{ampl}}{\sigma_0}\right] \left(\exp\left[\frac{4\sigma_{ampl}}{\sigma_0}\right] - \exp\left[\frac{3\sigma_{ampl}}{\sigma_0}\right]\right) \end{aligned} \quad (25)$$

The sum of these three parts gives the total amount of plastic strain accumulated during a single cycle of a triangular wave:

$$\begin{aligned}\Delta\epsilon_{pl,cyclic} &= \Delta\epsilon_{pl,1} + \Delta\epsilon_{pl,2} + \Delta\epsilon_{pl,3} \\ &= \dot{\epsilon}_{pl}(\sigma_{mean}) \frac{\sigma_0}{f\sigma_{ampl}} \sinh\left(\frac{\sigma_{ampl}}{\sigma_0}\right) \end{aligned} \quad (26)$$

Now, the plastic strain that is accumulated during one cycle of a triangular stress signal can be compared to the plastic strain developed by its static mean stress, using $f = 1/t_{cycle}$. This gives the acceleration factor of a triangular wave:

$$a_{tria} = \frac{\Delta\epsilon_{pl,cyclic}}{\Delta\epsilon_{pl,static}} = \frac{\Delta\epsilon_{pl,cyclic}}{\dot{\epsilon}_{pl}(\sigma_{mean})t_{cycle}} = \frac{\sinh\left(\frac{\sigma_{ampl}}{\sigma_0}\right)}{\frac{\sigma_{ampl}}{\sigma_0}} \quad (27)$$

Acceleration Factor of a Square Wave. To calculate the total accumulated plastic strain per cycle of a square wave, the stress signal is divided into two parts:

$$\begin{aligned} 0 \le t < \frac{1}{2f}: &\qquad \sigma = \sigma_{mean} + \sigma_{ampl} \\ \frac{1}{2f} \le t < \frac{1}{f}: &\qquad \sigma = \sigma_{mean} - \sigma_{ampl} \end{aligned} \quad (28)$$

where f is the frequency, σ_{mean} is the mean stress, and σ_{ampl} is the stress amplitude.

For each part, the accumulated plastic strain can be determined by integration of eq 20:

$$\Delta\epsilon_{pl,1} = \int_0^{1/2f} \frac{1}{2A_{rej}} \exp\left[\frac{\sigma_{mean} + \sigma_{ampl}}{\sigma_0}\right] \frac{1}{2f} \quad (29)$$

$$\Delta\epsilon_{pl,2} = \int_{1/2f}^{1/f} \frac{1}{2A_{rej}} \exp\left[\frac{\sigma_{mean} - \sigma_{ampl}}{\sigma_0}\right] \frac{1}{2f} \quad (30)$$

The sum of these two parts gives the total amount of plastic strain accumulated during a single cycle of a square wave:

$$\Delta\epsilon_{pl,cyclic} = \Delta\epsilon_{pl,1} + \Delta\epsilon_{pl,2} = \frac{\dot{\epsilon}_{pl}(\sigma_{mean})}{f} \cosh\left(\frac{\sigma_{ampl}}{\sigma_0}\right) \quad (31)$$

Now, the plastic strain that is accumulated during one cycle of a square stress signal can be compared to the plastic strain developed by its static mean stress, using $f = 1/t_{cycle}$. This gives the acceleration factor of a square wave:

$$a_{sq}(\sigma_{ampl}) = \frac{\Delta\epsilon_{pl,cyclic}}{\Delta\epsilon_{pl,static}} = \frac{\Delta\epsilon_{pl,cyclic}}{\dot{\epsilon}_{pl}(\sigma_{mean})t_{cycle}} = \cosh\left(\frac{\sigma_{ampl}}{\sigma_0}\right) \quad (32)$$

References and Notes

(1) Haward, R.; Thackray, G. *Proc. R. Soc. London A* **1968**, *302*, 453–472.
(2) Boyce, M. C.; Parks, D. M.; Argon, A. S. *Mech. Mater.* **1988**, *7*, 15–33.
(3) Wu, P. D.; van der Giessen, E. *J. Mech. Phys. Solids* **1993**, *41*, 427–456.
(4) Buckley, C. P.; Jones, D. C. *Polymer* **1995**, *36*, 3301–3312.
(5) Govaert, L. E.; Timmermans, P. H. M.; Brekelmans, W. A. M. *J. Eng. Mater. Technol.* **2000**, *122*, 177–185.
(6) Boyce, M. C.; Arruda, E. M.; Jayachandran, R. *Polym. Eng. Sci.* **1994**, *34*, 716–725.
(7) Wu, P. D.; van der Giessen, E. *Int. J. Solids Struct.* **1993**, *31*, 1493–1517.
(8) Wu, P. D.; van der Giessen, E. *Int. J. Plast.* **1993**, *11*, 211–235.
(9) van Melick, H. G. H.; Govaert, L. E.; Meijer, H. E. H. *Polymer* **2003**, *44*, 3579–3591.
(10) Meijer, H. E. H.; Govaert, L. E.; Smit, R. J. M. Multi-Level Finite Element Method for Modelling Rubber-Toughened Amorphous Polymers. In *Toughening of Plastics*; Pearson, R. A., Ed.; American Chemical Society: Washington, DC, 1999.
(11) Smit, R. J. M.; Brekelmans, W. A. M.; Meijer, H. E. H. *J. Mater. Sci.* **2000**, *35*, 2855–2867.
(12) Klompen, E. T. J.; Engels, T. A. P.; van Breemen, L. C. A.; Schreurs, P. J. G.; Govaert, L. E.; Meijer, H. E. H. *Macromolecules* **2005**, *38*, 7009–7017.
(13) Janssen, R. P. M.; de Kanter, D.; Govaert, L. E.; Meijer, H. E. H. *Macromolecules* **2008**, *41*, 2520–2530.
(14) Klompen, E. T. J.; Engels, T. A. P.; Govaert, L. E.; Meijer, H. E. H. *Macromolecules* **2005**, *38*, 6997–7008.
(15) Crissman, J. M.; McKenna, G. B. *J. Polym. Sci., Polym. Phys.* **1987**, *25*, 1667–1677.
(16) Crissman, J. M.; McKenna, G. B. *J. Polym. Sci., Polym. Phys.* **1990**, *28*, 1463–1473.
(17) Tobolsky, A.; Eyring, H. *J. Chem. Phys.* **1943**, *11*, 125–134.
(18) Coleman, B. D. *J. Polym. Sci.* **1956**, *20*, 447–455.
(19) Bueche, F. *J. Appl. Phys.* **1957**, *28*, 784–787.
(20) Zhurkov, S. N. *Int. J. Fract. Mech.* **1965**, *1*, 311–323.
(21) Matz, D. J.; Guldemond, W. G.; Cooper, S. L. *J. Polym. Sci., Polym. Phys.* **1972**, *10*, 1917–1930.
(22) Bauwens-Crowet, C.; Ots, J.-M.; Bauwens, J.-C. *J. Mater. Sci. Lett.* **1974**, *9*, 1197–1201.
(23) Regel, V. R.; Leksovsky, A. M. *Int. J. Fract.* **1967**, *3*, 99–109.
(24) McKenna, G. B.; Penn, R. W. *Polymer* **1980**, *21*, 213–220.
(25) Lesser, A. J. *Encycl. Polym. Sci. Technol.* **2002**, *6*, 197–251.
(26) Gotham, K. V. *Dev. Plast. Technol.* **1986**, *16*, 155–201.
(27) Trantina, G. G. *Polym. Eng. Sci.* **1984**, *24*, 1180–1184.

(28) Zhou, Y.; Brown, N. *J. Polym. Sci., Part B: Polym. Phys.* **1992**, *30*, 477–487.
(29) Roetling, J. *Polymer* **1965**, *6*, 311–317.
(30) Ree, T.; Eyring, H. *J. Appl. Phys.* **1955**, *26*, 793–800.
(31) van Melick, H. G. H.; Govaert, L. E.; Meijer, H. E. H. *Polymer* **2003**, *44*, 2493–2502.
(32) Zilvar, V. *Plast. Polym.* **1971**, *39*, 328–332.
(33) Bouda, V.; Zilvar, V.; Staverman, J. A. *J. Polym. Sci., Polym. Phys. Ed.* **1976**, *14*, 2313–2323.
(34) Li, X.; Hristov, H. A.; Yee, A. F.; Gidley, D. W. *Polymer* **1995**, *36*, 759–765.
(35) Szocs, F.; Klimová, M. *Eur. Polym. J.* **1996**, *32*, 1087–1089.
(36) Szocs, F.; Klimová, M.; Bartos, J. *Polym. Degrad. Stab.* **1997**, *55*, 233–235.
(37) Dixon, S. R.; Hill, A. J.; O'Donnell, J. A. *Polym. Degrad. Stab.* **2005**, *89*, 208–219.
(38) Struik, L. C. E. *Polymer* **1987**, *28*, 1521–1533.
(39) Read, B. E.; Dean, G. D.; Tomlins, P. E. *Polymer* **1988**, *29*, 2159–2169.
(40) Read, B. E.; Tomlins, P. E.; Dean, G. D. *Polymer* **1990**, *31*, 1204–1215.
(41) Koo, G. P.; Roldan, L. G. *J. Polym. Sci., Part A2* **1972**, *10*, 1145–1152.
(42) Takahara, A.; Yamada, K.; Kajiyama, T.; Takayanagi, M. *J. Appl. Polym. Sci.* **1980**, *25*, 597–614.
(43) Takahara, A.; Yamada, K.; Kajiyama, T.; Takayanagi, M. *J. Appl. Polym. Sci.* **1981**, *26*, 1085–1104.
(44) Sakurai, S.; Nokuwa, S.; Morimoto, M.; Shibayama, M.; Nomura, S. *Polymer* **1994**, *35*, 532–539.
(45) Lesser, A. J. *J. Appl. Polym. Sci.* **1995**, *58*, 869–879.
(46) Jones, N. A.; Lesser, A. J. *J. Polym. Sci., Polym. Phys. Ed.* **1998**, *36*, 2751–2760.
(47) Nishimura, H.; Narisawa, I. *Polym. Eng. Sci.* **1991**, *31*, 399–403.
(48) Riddel, M. N.; Koo, G. P.; O'Toole, J. L. *Polym. Eng. Sci.* **1966**, *6*, 363–368.
(49) Constable, I.; Williams, J. G.; Burns, D. J. *J. Mech. Eng. Sci.* **1970**, *12*, 20–29.
(50) Crawfordzp, R. J.; Benham, P. P. *J. Mater. Sci.* **1974**, *9*, 18–28.
(51) Crawford, R. J.; Benham, P. P. *Polymer* **1974**, *16*, 908–914.
(52) Sauer, J. A.; Foden, E.; Morrow, D. R. *Polym. Eng. Sci.* **1977**, *17*, 246–250.
(53) Rittel, D. *Mech. Mater.* **2000**, *32*, 131–147.
(54) Tauchert, T. R. *Int. J. Eng. Sci.* **1967**, *5*, 353–365.
(55) Tauchert, T. R.; Afzal, S. M. *J. Appl. Phys.* **1967**, *38*, 4568–4572.
(56) Justice, L. A.; Schultz, J. M. *J. Mater. Sci. Lett.* **1980**, *15*, 1584–1585.
(57) Sherby, O. D.; Dorn, J. E. *J. Mech. Phys. Solids* **1958**, *6*, 145–162.
(58) Ward, I. M.; Wilding, M. A. *J. Polym. Sci., Polym. Phys. Ed.* **1984**, *22*, 561–575.

MA071274A